Anomalous damping dependence of the switching time in Fe/FePt bilayer recording media

Razvan-V. Ababei,[1] Matthew O. A. Ellis,[2] Richard F. L. Evans,[1] and Roy W. Chantrell[1]
[1]*Department of Physics, The University of York, Heslington, York YO10 5DD, United Kingdom*
[2]*School of Physics and CRANN, Trinity College, Dublin 2, Ireland*

(Received 26 October 2018; revised manuscript received 12 December 2018; published 24 January 2019)

Gilbert damping plays a significant role in magnetic reversal processes, and it determines the timescale of the switching. Here we investigate the properties of exchange-coupled composite media and the dependence of the switching time on the damping constant of the soft layer using atomistic spin dynamics. For a bilayer Fe/FePt medium, we find an anomalous increase of the switching time with increasing soft layer damping constant. The reversal occurs via a high-temperature exchange spring, and we show that the increase in the switching time is related to a corresponding increase in the time to establish the exchange spring. This phenomenon is delicately balanced in that the switching time increase occurs only in fields close to the coercivity.

DOI: 10.1103/PhysRevB.99.024427

I. INTRODUCTION

Magnetic recording has seen a rapid increase in areal density in the past few decades driven by an increasing consumer demand for data storage. The increase in areal density has been achieved through a scaling approach whereby the grain size is reduced in order to maintain a high signal-to-noise ratio (SNR) at high densities, while the magnetocrystalline anisotropy of the grains has been increased in order to maintain thermal stability of written information. However, this approach is limited due to the fact that increased anisotropy gives rise to larger write field requirements, which are approaching the limits of available write fields using current inductive technology. This is formalized in the magnetic recording trilemma [1].

One of the most promising strategies to solve the trilemma is heat-assisted magnetic recording (HAMR) [2,3]. This uses localized heating via a laser to induce a transient reduction of the anisotropy, thereby allowing magnetization reversal, while thermal stability is established on reduction of the temperature back to ambient. To achieve writing at sufficiently low temperatures, a medium with low Curie temperature and high anisotropy is required. The $L1_0$ phase of FePt is currently the preferred option, with recording densities greater than those of conventional perpendicular magnetic recording having been demonstrated by Ju *et al.* [4]. However, the high temperatures of the HAMR process lead to enhanced noise and reliability problems, and advanced designs of composite media are being considered in order to reduce the writing temperature. One option is to combine the high anisotropy material with one that has a higher Curie temperature but a lower anisotropy to trigger magnetization reversal through a high-temperature exchange spring. Such structures are known as exchange-coupled composite (ECC) media [5]. By combining a soft Fe layer on top of the hard FePt layer, it has been shown in previous studies that ECC media can reduce thermal error and achieve switching at lower temperatures [6–8]. The ECC medium design is capable of reducing the noise, known as jitter, during the writing process by increasing the average polarization of the magnetic grain using high M_S layers with high Curie temperature.

Of particular interest is the switching dynamics and the ultimate speed at which the magnetization reversal can take place. Kikuchi [9] showed that the switching time of a single domain is given by

$$\tau \propto \frac{1+\alpha^2}{\alpha H}, \tag{1}$$

where α is the Gilbert damping constant and H is the applied field. Equation (1) gives a minimum switching time for $\alpha = 1$. For most materials $\alpha \ll 1$, and it is expected that the switching time will decrease with increasing damping. By varying the damping, it is therefore possible to control the switching time in recording media.

Here we investigate the dynamical reversal process using an atomistic spin model, showing an unexpected increase of the switching time with increasing damping of the soft phase. This is ascribed to high-angle precession at low damping setting up more rapidly the exchange spring condition, which initiates the reversal of the FePt layer. The effect is found to depend strongly on the magnitude of the switching field. We conclude that advanced media designs require a detailed analysis of the reversal mechanism since the damping dependence may not apply in all cases.

II. ATOMISTIC MODEL OF ECC MEDIA

In the following, we present an atomistic model of ECC media as a combination of two exchange-coupled magnetic phases, specifically a hard and soft phase represented by FePt and Fe, respectively.

We model a cylindrical bilayer grain, with a total height of 10 nm and a basal diameter of 5 nm, comprised of layers of FePt and Fe, each of 5 nm thickness, coupled by a ferromagnetic interface exchange. The magnetic properties of the system have been simulated using an atomistic spin model as implemented in the VAMPIRE software package [10]. Atomistic modeling is important in terms of a physical

understanding of the dynamical properties at elevated temperatures because the temperature dependence of the anisotropy and importantly the interlayer exchange arises naturally in the model results. In this model, the energy is expressed at the atomistic level within the localized atomic spin moment assumption as

$$\begin{aligned}\mathcal{H} = &-\sum_{i,j} J_{ij}^{\mathrm{Fe}} \mathbf{S}_i^{\mathrm{Fe}} \cdot \mathbf{S}_j^{\mathrm{Fe}} - \sum_i k_u^{\mathrm{Fe}} \left(S_{iz}^{\mathrm{Fe}}\right)^2 \\ &- \sum_{i,j} J_{ij}^{\mathrm{FePt}} \mathbf{S}_i^{\mathrm{FePt}} \cdot \mathbf{S}_j^{\mathrm{FePt}} - \sum_i k_u^{\mathrm{FePt}} \left(S_{iz}^{\mathrm{FePt}}\right)^2 \\ &- \sum_{i,j} J_{ij}^{\mathrm{int}} \mathbf{S}_i^{\mathrm{Fe}} \cdot \mathbf{S}_j^{\mathrm{FePt}} - \sum_i \mu_0 \mu_i \mathbf{S}_i \cdot \mathbf{H}_{\mathrm{app}}. \end{aligned} \tag{2}$$

Here, the spins are represented as unit vectors, $\mathbf{S}_i$, with the magnitude of the magnetic moment given by μ_i, and μ_0 is the permeability of free space. J_{ij} represents the exchange coupling, which is restricted to the nearest neighbors, and k_u is the on-site uniaxial anisotropy constant. For Fe the exchange value is $J_{ij}^{\mathrm{Fe}} = 7.05 \times 10^{-21}$ J, and for FePt $J_{ij}^{\mathrm{FePt}} = 4.5 \times 10^{-21}$ J. The Fe magnetic moment in the soft layer is taken as $2.2\mu_B$, while within the FePt layer *ab initio* calculations [11] have shown an effective Fe moment of $2.86\mu_B$ and $0.36\mu_B$ for Pt in bulk systems. However, in nanoscale systems the magnitude of the Fe moment drops substantially at surfaces or interfaces, therefore we use a combined effective FePt moment of $1.9\mu_B$, which corresponds to a macroscopic saturation magnetization of 1024 emu/cm^3 [12].

Ab initio studies by Mryasov *et al.* [13] found that the large anisotropy of FePt ($K \approx 10^8$ erg/cm^3 [14]) arises from the hybridization of the Fe and Pt orbitals. Mryasov *et al.* proposed an effective spin Hamiltonian where the induced Pt moments are accounted for through a long-range mediated exchange interaction and anisotropy contributions from single- and two-ion terms. For computational efficiency, here we use an equivalent nearest-neighbor exchange and single ion uniaxial form for the anisotropy of FePt with an atomistic anisotropy constant of $k_u^{\mathrm{FePt}} = 2.2 \times 10^{-22}$ J and $k_u^{\mathrm{Fe}} = 5.65 \times 10^{-25}$ J for Fe arranged in a body-centered-cubic (bcc) structure with a lattice parameter equal to 3.249 Å for FePt. Since we are interested in determining basic reversal mechanisms, this is not expected to alter the essential predictions.

The simulations we present in this paper involve the calculation of dynamic magnetic properties, therefore we use the stochastic Landau-Lifshitz-Gilbert (LLG) equation in order to describe the dynamics of the spins. This allows the simulation of thermally induced magnetization changes and also the time dependence of the coercivity [15]. The stochastic LLG equation is

$$\frac{\partial \mathbf{S}_i}{\partial t} = -\frac{\gamma}{1+\lambda_i^2} \mathbf{S}_i \times [\mathbf{H}_i + \lambda_i (\mathbf{S}_i \times \mathbf{H}_i)], \tag{3}$$

where the parameter λ_i represents the coupling to the heat bath at the atomistic level. Formally, we choose this description to represent the intrinsic damping, since this differs from the macroscopic Gilbert damping, which includes the effects of magnon contributions to the damping that naturally occur in the atomistic approach. $\mathbf{H}_i = -(1/\mu_0\mu_i)\partial\mathcal{H}/\partial\mathbf{S}_i + \mathbf{H}_{\mathrm{th}}^i$ is the internal effective field, where $\mathbf{H}_{\mathrm{th}}^i$ is the thermal field at each site. The magnitude of $\mathbf{H}_{\mathrm{th}}^i$ is determined using the fluctuation-dissipation theorem [16]. Further details of the atomistic spin dynamics method are described in Ref. [10].

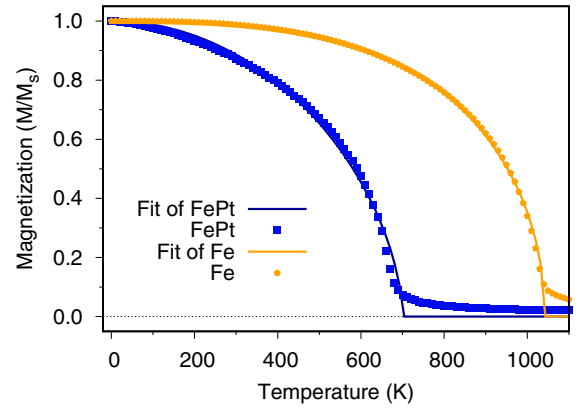

FIG. 1. Calculated temperature-dependent magnetization for Fe and FePt using Monte Carlo simulations. The solid lines represent the fitting using the following expression: $M(T) = M_0[1 - (T/T_C)^{\alpha}]^{\beta}$, which gives a Curie temperature of 1050 K for Fe and 700 K for FePt.

Atomistic simulations are classical in nature and do not reproduce the exact experimental form of $M(T)$. Evans *et al.* [17] developed a simple temperature rescaling approach by considering classical and quantum spin-wave fluctuations, and it provides quantitative agreement of the temperature-dependent magnetization between atomistic simulations and experiment. The scaling law is of the form

$$M(\tau) = M_0(1 - \tau^{\alpha})^{\beta}, \tag{4}$$

where M_0 is the saturation magnetization at 0 K, $\tau = T/T_C$ is the reduced temperature, $\beta \approx 1/3$ is the magnetization critical exponent, and α is the rescaling exponent. The aim of this rescaling is to give more quantitative predictions of the temperature-dependent magnetization. Therefore, by using a rescaled simulation temperature following $\tau_{\mathrm{sim}} = \tau_{\mathrm{exp}}^{\alpha}$, we can obtain a temperature-dependent magnetization similar to experiment. In Ref. [17] the rescaling exponent for Fe was found to be 2.86, which gives a more accurate dependence of the temperature-dependent curve as shown in Fig. 1. For FePt we found an appropriate rescaling factor of 1.5, which gives a Curie temperature of 700 K.

The damping constant plays a major role in the spin dynamics, and it can vary with a number of parameters such as the size of the magnetic grains, crystal ordering, defects, and impurities. FePt exhibits a large damping constant as shown experimentally by Becker *et al.* [18]. Their measurements show a value of FePt damping around 0.1 with high accuracy and good stability over a wide range of temperatures. Thus, this value will be assumed in our further simulations in this paper. FePt has a large effective damping constant [18], largely due to extrinsic processes [19]. However, the damping constant in Fe can be increased significantly from its low intrinsic value by doping with rare-earth (RE) metals. This has the potential for increasing the switching speed as shown in Eq. (1). The effect of RE doping in permalloy has been shown

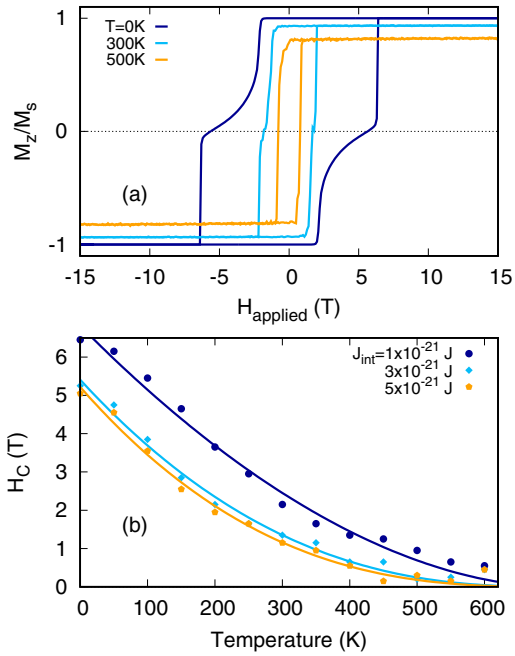

FIG. 2. The temperature dependence of the coercive field for ECC media. Graph (a) illustrates a series of hysteresis loops for ECC media at different temperatures below the Curie point for an interface exchange constant of $J_{\text{int}} = 1 \times 10^{-21}$ J. In graph (b) the coercivity has been extracted from the temperature-dependent hysteresis loops for three different values of the interface exchange constant. The solid lines are fits using Eq. (5) for each interface exchange constant.

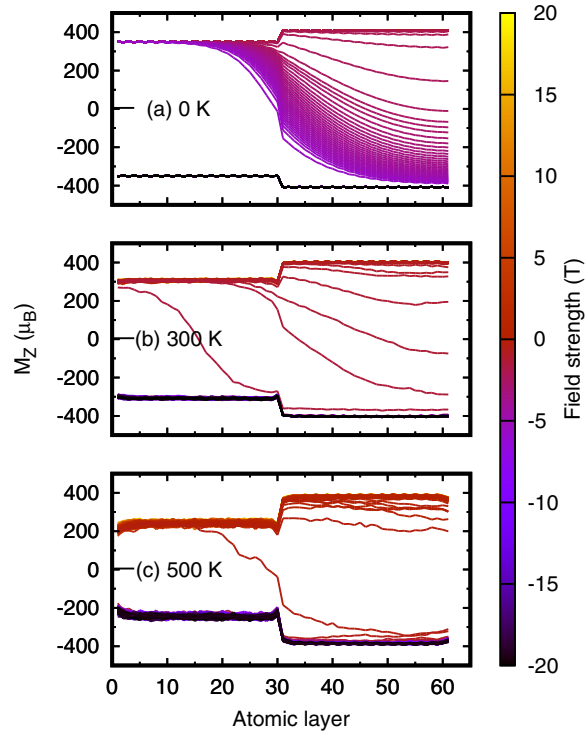

FIG. 3. Plot of the magnetization for each atomic layer. The total height of the ECC media grain is 10 nm, which contains 60 atomic layers. The first 30 layers correspond to FePt, and the layers between 30 and 60 correspond to Fe. The applied field varies from 20 to −20 T representing the first part of the hysteresis loop.

in Ref. [20], where the damping constant varies linearly with the concentration of RE.

III. MAGNETIZATION REVERSAL AT FINITE TEMPERATURE

We first investigate the temperature dependence of the coercivity by simulating a series of hysteresis loops at different temperatures. Each loop is simulated over 60 ns using an integration time step of 0.1 fs, and the applied field is varied in increments of 0.1 T every 0.1 ns. These loops are shown in Fig. 2(a) with an interface exchange of $J_{\text{int}} = 1.5 \times 10^{-21}$ J. At low temperatures, it is clear that switching is a two-step process where the soft Fe layer switches with a small field while the FePt layer requires a much larger (≈6.82 T) field to switch. As the temperature increases, there is a transition from this two-step process to a single step due a decrease in the FePt anisotropy relative to the interface exchange. This reduction in the coercivity agrees well with experimental measurements, which observed that the coercivity is reduced to approximately half with an equal thickness of Fe on top of $L1_0$ FePt [21]. At each temperature, the coercive field has been extracted, which is shown in Fig. 2(b). This shows a clear decrease with increasing temperature, which can be modeled using a power-law expression,

$$H_C(T) = H_C(0)\left(1 - \frac{T}{T_C}\right)^{\epsilon}, \tag{5}$$

where ϵ is the exponent factor and $H_C(0)$ is the coercive field at 0 K. We find an increase of the exponent ϵ from 1.68 for $J_{\text{int}} = 1 \times 10^{-21}$ J to 2.69 for $J_{\text{int}} = 5 \times 10^{-21}$ J, denoting lower coercivity for a stronger coupling at the interface. In particular, we note the coercive field at 0 K decreases for larger J_{int} from 6.82 T for $J_{\text{int}} = 1 \times 10^{-21}$ J to 5.41 T for $J_{\text{int}} = 3 \times 10^{-21}$ J, and 5.40 T for $J_{\text{int}} = 5 \times 10^{-21}$ J. For a typical value of the interface exchange coupling of $J_{\text{int}} = 1 \times 10^{-21}$ J, the coercive field at 500 K is 0.95 T, which is feasible for switching with the existing inductive head technology.

With the static properties of the switching mechanism established, we now proceed to study the localized behavior in detail to determine the precise reversal mechanism. The results are shown in Fig. 3, which shows the evolution of the layer-resolved magnetization during the first branch of the hysteresis loop where the magnetic-field strength varies from 20 T to −20 T. As before, the field is increased at a rate of 1 T/ns, which gives an approximate timescale for the switching. At zero field there is a discontinuity of the magnetization at the interface due to the different saturation magnetization of each magnetic phase. Due to a higher M_S of the soft layer, an accentuated spring effect occurs during the switching process. A particular aspect related to the temperature dependence of the speed of domain-wall propagation can be seen in Fig. 3. Slower switching is observed to occur at 0 K [panel (a)] in comparison with higher temperatures [panel (c)] since the domain wall is strongly pinned at the interface due to the high anisotropy, as expected from the prediction of Kronmüller

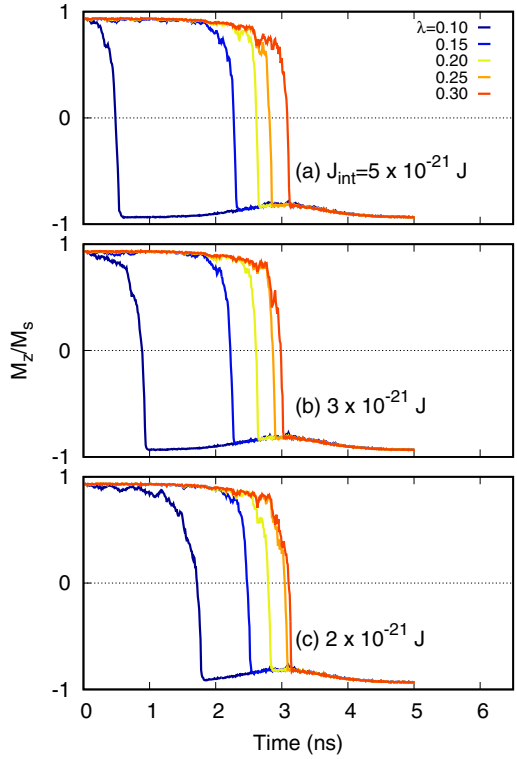

FIG. 4. Calculated evolution of z-components of reduced magnetization during the reversal mechanism for different interface exchange coupling strength (a) $J_{\text{int}} = 5 \times 10^{-21}$ J, (b) $J_{\text{int}} = 3 \times 10^{-21}$ J, and (c) $J_{\text{int}} = 2 \times 10^{-21}$ J with a variation of damping of the soft layer (Fe). The damping constant of the hard phase (FePt) has been kept fixed at 0.1.

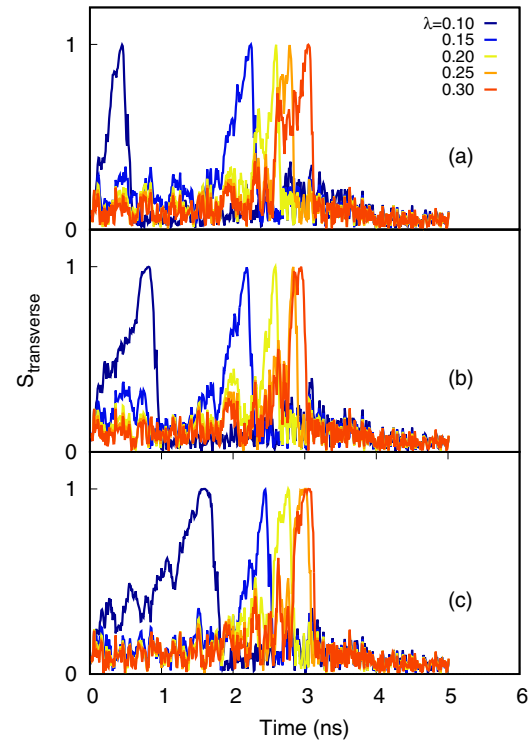

FIG. 5. Calculated evolution of the transverse component of the reduced magnetization of the Fe layer as $S^{\text{Fe}}_{\text{transverse}} = \frac{1}{N}\sum_i^N \sqrt{(S^{\text{Fe}}_{ix})^2 + (S^{\text{Fe}}_{iy})^2}$ during the reversal mechanism for different interface exchange coupling strength (a) $J_{\text{int}} = 5 \times 10^{-21}$ J, (b) $J_{\text{int}} = 3 \times 10^{-21}$ J, and (c) $J_{\text{int}} = 2 \times 10^{-21}$ J with a variation of damping of the soft layer (Fe). The damping constant of the hard phase (FePt) has been kept fixed at 0.1.

and Goll [22]. At elevated temperatures, the weaker pinning leads to faster domain-wall motion and reduced switching fields, indicative of a temperature-enhanced exchange spring effect. The exchange spring effect leads to a reduction in the coercivity, as shown in Fig. 2.

IV. IMPACT OF DAMPING ON THE REVERSAL MECHANISM

We now proceed to investigate the effect of the damping of the soft layer on the ECC reversal mechanism in a HAMR-like experiment. To investigate the physics of the HAMR process, a simplified model is used by applying simultaneously a constant reversing magnetic field aligned along the $-z$ direction and a Gaussian heat profile given by

$$T(t) = (T_{\max} - T_{\min}) \exp\left[-\left(\frac{t - t_p}{t_c}\right)^2\right] + T_{\min}, \qquad (6)$$

where t_c is the cooling time and t_p is the time at which the temperature reaches its maximum $T_{\max}$. The total time of each simulation is 5 ns with the temperature peak at $t_p = 3$ ns and a cooling time of $t_c = 1$ ns. The minimum and maximum temperatures used are 300 and 500 K, respectively.

We distinguish two cases of the reversal mechanism depending on the strength of the external magnetic field. The first case corresponds to the maximum likely reversing field from inductive technology of 1 T. As has been shown in the previous section, this value is close to the coercivity of ECC media at the maximum temperature of the heat pulse (500 K). In this region, the reversal mechanism is found to be very sensitive to the damping parameter. In particular, we observed an unexpected increase of the switching time with an increased damping, as shown in Fig. 4. This is clearly inconsistent with the switching time expected for a single domain switching given by Eq. (1). The second case is when the reversing field is much larger than the coercivity, which, as shown later, presents a decrease in the switching time with increasing damping.

For the first case, we interpret this behavior in terms of the exchange spring mechanism of magnetization switching. The presence of the exchange spring mechanism is confirmed in Fig. 3, which shows that reversal proceeds via nucleation of a domain in the Fe, which is first pinned at the FePt/Fe interface before propagating into the FePt. The switching speed depends on the pinning strength, determined by the anisotropy and interface exchange coupling and also, crucially, by the time needed to establish the spring configuration. In Fig. 4 it can be seen that, for low damping, the switching time increases with decreasing exchange, presumably as a result of the increasing pinning field. However, at higher damping this trend is lost as the switching time becomes dominated by the time needed to establish the exchange spring. This is

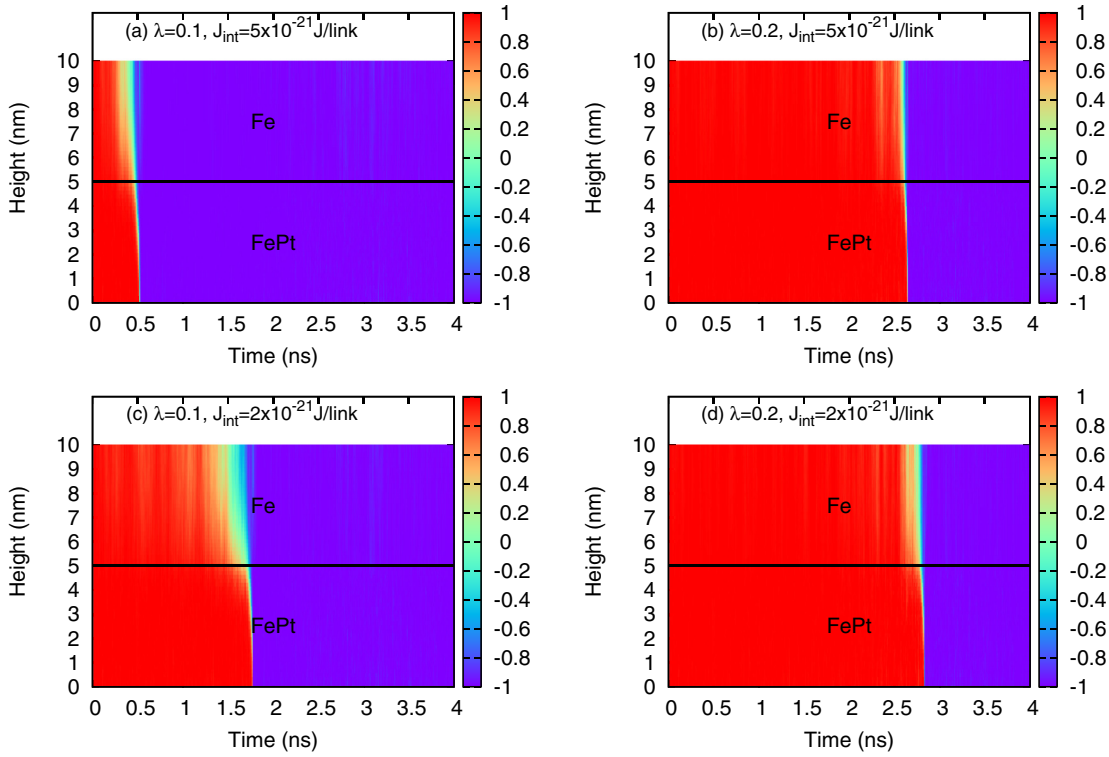

FIG. 6. The magnetization profile during the reversal mechanism for two different exchange couplings and two different Gilbert damping values. The system contains 60 atomic layers; the first 30 layers ≈5 nm correspond to FePt, and the top layers correspond to Fe. The colors indicate the value of the z-component of magnetization. Here red indicates a positive value of reduced magnetization on the z direction, blue indicates a negative value, and white suggests a plane orientation of the reduced magnetization.

demonstrated in Fig. 5, which shows the time evolution of the transverse component of the magnetization of the Fe layer: the slowing down of the development of the exchange spring is clear.

Figure 6 shows four different examples of the reversal mechanism with two different values of damping and exchange-coupling values at the interface. The reduced z-component of the magnetization has been averaged for each atomic layer and plotted as a function of height and time. The white color denotes an in-plane orientation of the magnetization, indicating that the switching requires high-angle precession of the Fe. More cycles of precession can be seen for lower damping of the soft phase as shown in Figs. 6(a) and 6(b). It can be seen that the switching speed increases with increasing interface exchange coupling, the effect being most pronounced for the case of lower damping ($\lambda = 0.1$).

Figure 7(a) shows how the average reversal time, which is defined as the time taken for the z-component of the magnetization to align in-plane [23], depends on the damping parameter for different interface exchange-coupling values. As discussed earlier, increasing the damping leads to a monotonic increase of the reversal time, while stronger interface exchange coupling accelerates the spring behavior of the soft phase over the hard phase, in strong agreement with the Landau-Lifshitz-Bloch macrospin model demonstrated by Vogler *et al.* [24]. Moreover, stronger coupling leads to a more accentuated impact of the damping constant over the reversal time, suggested by the shape of the curves corresponding to each coupling value.

This low damping exchange spring mechanism is observed to be sensitive to the reversing field relative to the coercivity of the system. Figure 7(b) shows that fields greater than 2 T

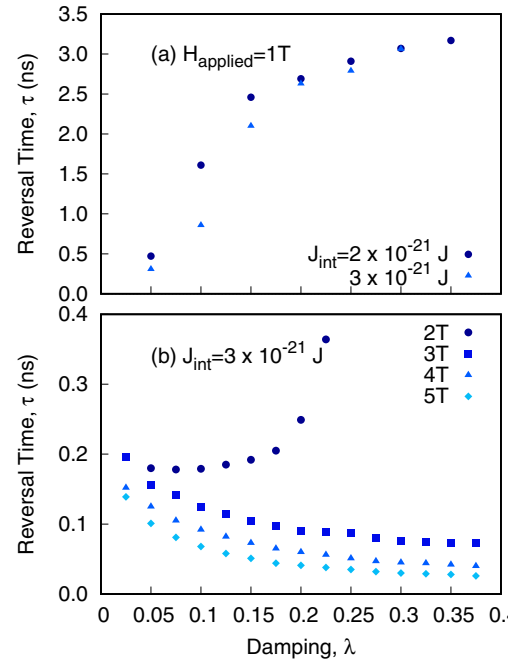

FIG. 7. The dependence of reversal time as a function of damping parameter for different cases: (a) low field near the coercivity, $H_{\text{applied}} = 1$ T, and (b) higher fields.

lead to a reduction of the reversal time. In this region, a clear decrease of the switching time with damping can be observed, as expected from Eq. (1). These fields are higher than the room-temperature coercivity, as shown in Fig. 2, so the reversal is essentially coherent; the exchange spring does not develop and the reversal time depends conventionally on the damping.

The thickness of the soft Fe layer is expected to play a crucial role in the reversal mechanism since it will first change the switching field of the sample, and secondly it will affect the formation of the exchange spring. In the limit of small thickness, the Fe will tend to reverse as a single domain. It is also worth noting that the choice of a peak temperature below the FePt T_C means that both layers are substantially magnetized during the switching process, which causes the domain wall to form. Higher temperatures lead to higher domain-wall mobility and lower anisotropy in the FePt, leading to faster switching in general.

V. CONCLUSIONS AND OUTLOOK

In conclusion, we have investigated the temperature-dependent magnetic response of ECC HAMR media using an atomistic spin model using the VAMPIRE code. The reversal process was investigated by calculating temperature-dependent hysteresis loops. It was found that reversal proceeded via an exchange spring mechanism that was enhanced at elevated temperatures due to the reduction of the anisotropy and consequently the pinning field. A simple model of the HAMR process was then constructed using a constant applied field and a Gaussian time-dependent temperature profile. We used this procedure to investigate the dependence of the switching time on the damping constant of the Fe layer. For the case of a reversing field of 1 T, an unexpected increase of switching time with increased damping constant was observed. This effect was shown to be due to the increase of the time needed to establish the exchange spring with increasing damping constant. Interestingly, upon increasing the reversing field, the expected decrease of the switching time with increased damping was recovered. However, 1 T is at the limit of inductive technology, which suggests that the effect presented here could be an important factor in the design of advanced media for HAMR.

ACKNOWLEDGMENTS

The authors are grateful to Advanced Storage Technology Consortium (ASTC) for financial support, and special thanks go to Alexandru Stancu for helpful discussions.

[1] H. Richter and A. Y. Dobin, J. Magn. Magn. Mater. **287**, 41 (2005).
[2] R. MacDonald and J. Beck, J. Appl. Phys. **40**, 1429 (1969).
[3] R. E. Rottmayer, S. Batra, D. Buechel, W. A. Challener, J. Hohlfeld, Y. Kubota, L. Li, B. Lu, C. Mihalcea, K. Mountfield *et al.*, IEEE Trans. Magn. **42**, 2417 (2006).
[4] G. Ju, Y. Peng, E. K. C. Chang, Y. Ding, A. Q. Wu, X. Zhu, Y. Kubota, T. J. Klemmer, H. Amini, L. Gao, Z. Fan, T. Rausch, P. Subedi, M. Ma, S. Kalarickal, C. J. Rea, D. V. Dimitrov, P. Huang, K. Wang, X. Chen, C. Peng, W. Chen, J. W. Dykes, M. A. Seigler, E. C. Gage, R. Chantrell, and J. Thiele, IEEE Trans. Magn. **51**, 1 (2015).
[5] D. Suess, J. Lee, J. Fidler, and T. Schrefl, J. Magn. Magn. Mater. **321**, 545 (2009); P. Esquinazi, J. Barzola-Quiquia, D. Spemann, M. Rothermel, H. Ohldag, N. García, A. Setzer, T. Butz, *ibid.* **322**, 1156 (2010).
[6] D. Suess and T. Schrefl, Appl. Phys. Lett. **102**, 162405 (2013).
[7] T. Dutta, S. N. Piramanayagam, M. S. M. Saifullah, and C. S. Bhatia, Appl. Phys. Lett. **111**, 042405 (2017).
[8] O. Hellwig, J. B. Kortright, K. Takano, and E. E. Fullerton, Phys. Rev. B **62**, 11694 (2000).
[9] R. Kikuchi, J. Appl. Phys. **27**, 1352 (1956).
[10] R. F. L. Evans, W. J. Fan, P. Chureemart, T. A. Ostler, M. O. A. Ellis, and R. W. Chantrell, J. Phys.: Condens. Matter **26**, 103202 (2014).
[11] C. J. Aas, P. J. Hasnip, R. Cuadrado, E. M. Plotnikova, L. Szunyogh, L. Udvardi, and R. W. Chantrell, Phys. Rev. B **88**, 174409 (2013).
[12] D. Weller, A. Moser, L. Folks, and M. Best, IEEE Trans. Magn. **36**, 10 (2000).
[13] O. N. Mryasov, U. Nowak, K. Y. Guslienko, and R. W. Chantrell, Europhys. Lett. **69**, 805 (2005).
[14] D. Weller and A. Moser, IEEE Trans. Magn. **35**, 4423 (1999).
[15] M. O. A. Ellis, R. F. L. Evans, T. A. Ostler, J. Barker, U. Atxitia, O. Chubykalo-Fesenko, and R. W. Chantrell, Low Temp. Phys. **41**, 705 (2015).
[16] A. Lyberatos, D. V. Berkov, and R. W. Chantrell, J. Phys.: Condens. Matter **5**, 8911 (1993).
[17] R. F. L. Evans, U. Atxitia, and R. W. Chantrell, Phys. Rev. B **91**, 144425 (2015).
[18] J. Becker, O. Mosendz, D. Weller, A. Kirilyuk, J. C. Maan, P. C. M. Christianen, T. Rasing, and A. Kimel, Appl. Phys. Lett. **104**, 152412 (2014).
[19] N. Mo, J. Hohlfeld, M. ul Islam, C. S. Brown, E. Girt, P. Krivosik, W. Tong, A. Rebei, and C. E. Patton, Appl. Phys. Lett. **92**, 022506 (2008).
[20] G. Woltersdorf, M. Kiessling, G. Meyer, J.-U. Thiele, and C. H. Back, Phys. Rev. Lett. **102**, 257602 (2009).
[21] L. Liu, W. Sheng, J. Bai, J. Cao, Y. Lou, Y. Wang, F. Wei, and J. Lu, Appl. Surf. Sci. **258**, 8124 (2012).
[22] H. Kronmüller and D. Goll, Physica B **319**, 122 (2002).
[23] J. Barker, R. F. L. Evans, R. W. Chantrell, D. Hinzke, and U. Nowak, Appl. Phys. Lett. **97**, 192504 (2010).
[24] C. Vogler, C. Abert, F. Bruckner, and D. Suess, Phys. Rev. B **90**, 214431 (2014).